

OCTOBER 10 2018

## Diving behavior of Cuvier's beaked whales inferred from three-dimensional acoustic localization and tracking using a nested array of drifting hydrophone recorders

Jay Barlow; Emily T. Griffiths; Holger Klinck; Danielle V. Harris



*J. Acoust. Soc. Am.* 144, 2030–2041 (2018)

<https://doi.org/10.1121/1.5055216>



CrossMark



 **ASA**

Advance your science and career as a member of the **Acoustical Society of America**

[LEARN MORE](#)

# Diving behavior of Cuvier's beaked whales inferred from three-dimensional acoustic localization and tracking using a nested array of drifting hydrophone recorders

Jay Barlow<sup>a)</sup>

National Oceanic and Atmospheric Administration National Marine Fisheries Service, Southwest Fisheries Science Center, Marine Mammal and Turtle Division, 8901 La Jolla Shores Drive, La Jolla, California 92037, USA

Emily T. Griffiths<sup>b)</sup>

Ocean Associates, Inc., 4007 North Arlington Street, Arlington, Virginia 22207, USA

Holger Klinck

Bioacoustics Research Program, Cornell Laboratory of Ornithology, Cornell University, 159 Sapsucker Woods Road, Ithaca, New York 14850, USA

Danielle V. Harris

Centre for Research into Ecological and Environmental Modelling, The Observatory, Buchanan Gardens, University of St. Andrews, St. Andrews, Fife, KY16 9LZ, United Kingdom

(Received 10 April 2018; revised 1 August 2018; accepted 31 August 2018; published online 10 October 2018)

Echolocation pulses from Cuvier's beaked whales are used to track the whales' three-dimensional diving behavior in the Catalina Basin, California. In 2016, five 2-element vertical hydrophone arrays were suspended from the surface and drifted at ~100-m depth. Cuvier's beaked whale pulses were identified, and vertical detection angles were estimated from time-differences-of-arrival of either direct-path signals received on two hydrophones or direct-path and surface-reflected signals received on the same hydrophone. A Bayesian state-space model is developed to track the diving behavior. The model is fit to these detection angle estimates from at least four of the drifting vertical arrays. Results show that the beaked whales were producing echolocation pulses and are presumed to be foraging at a mean depth of 967 m (standard deviation = 112 m), approximately 300 m above the bottom in this basin. Some whales spent at least some time at or near the bottom. Average swim speed was  $1.2 \text{ m s}^{-1}$ , but swim direction varied during a dive. The average net horizontal speed was  $0.6 \text{ m s}^{-1}$ . Results are similar to those obtained from previous tagging studies of this species. These methods may allow expansion of dive studies to other whale species that are difficult to tag. <https://doi.org/10.1121/1.5055216>

[AMT]

Pages: 2030–2041

## I. INTRODUCTION

The detailed diving behavior of most whales is not directly observable by humans. Diving studies are especially challenging for deep-diving whales such as beaked whales (family Ziphiidae), for which each foraging dive can last more than two hours at depths of up to 3000 m (Schorr *et al.*, 2014). Most of what we currently know about beaked whale diving behavior comes from tagging studies. Time-depth recorders have been used to quantify dive times and depths, inter-dive periods, and descent and ascent rates (Tyack *et al.*, 2006; Baird *et al.*, 2008). Acoustic recording tags have added the ability to study details related to their foraging behavior (Johnson *et al.*, 2004; Tyack *et al.*, 2006). Multi-sensor tags that also include accelerometers and magnetic

headings allow even more detailed re-constructions of three-dimensional (3D) diving and foraging behavior (Johnson *et al.*, 2008; Laplanche *et al.*, 2015). However, tagging studies have been successfully applied to only a small subset of the 22 species of beaked whale.

One of the better studied species is Cuvier's beaked whale (*Ziphius cavirostris*), which have been tagged in the Mediterranean (Johnson *et al.*, 2004; Tyack *et al.*, 2006), Hawaii (Baird *et al.*, 2008), Southern California (DeRuiter *et al.*, 2013; Schorr *et al.*, 2014) and the Azores (Visser, 2017). In general, diving behaviors were similar in different areas. To summarize from those studies, Cuvier's beaked whales typically conduct deep foraging dives with mean durations of 60–70 min and with mean inter-deep-dive periods of 60–100 min. During a deep foraging dive, whales descend at a rate of  $\sim 1.4\text{--}1.5 \text{ m s}^{-1}$  to a depth of  $\sim 450 \text{ m}$  before initiating echolocation and foraging. Whales forage typically for  $\sim 35 \text{ min}$  at depths of 700–2000 m (and as deep as 3000 m) before returning to the surface. During their ascent, whales stop echolocation at a depth of  $\sim 850 \text{ m}$  and continue to ascend at a slower rate ( $0.6\text{--}0.7 \text{ m s}^{-1}$ ) than their descent. During inter-

<sup>a)</sup>Electronic mail: jay.barlow@noaa.gov

<sup>b)</sup>Also at: National Oceanic and Atmospheric Administration National Marine Fisheries Service, Marine Mammal and Turtle Division, Southwest Fisheries Science Center, 8901 La Jolla Shores Drive, La Jolla, CA 92037, USA.

deep-dive periods, whales make several shorter (15–21 min) dives to shallower depths and surface multiple times during relatively short (~2–3 min) surfacing series. The only other extensively tagged beaked whale species, Blainville's beaked whale (*Mesoplodon densirostris*), shows very similar behavior but generally has shorter foraging dives to shallower depths (Tyack *et al.*, 2006; Baird *et al.*, 2008).

Because beaked whales make regular echolocation pulses during foraging dives (Johnson *et al.*, 2004; Zimmer *et al.*, 2008), passive acoustic tracking is an alternative tool to study their diving behavior. To date, this approach has been largely limited to studies of sperm whales (*Physeter macrocephalus*). Large-aperture arrays of bottom-mounted, surface-suspended or towed hydrophones have been used to determine the 3D diving behavior of vocalizing sperm whales (Møhl *et al.*, 2000; Thode, 2004; Nosal and Frazer, 2007; Miller and Dawson, 2009; Baggenstoss, 2011). A key element to these studies is the localization of their echolocation pulses using time-difference-of-arrival (TDOA) of the sounds on multiple hydrophones. At sea, cabled hydrophone arrays are unwieldy at scales greater than a few hundred meters, so multiple autonomous recorders are often used to create larger aperture arrays. Maintaining recording synchrony is problematic for autonomous recorders because digital clocks with sufficient precision to accurately measure TDOA are not widely available in commercial recording systems. Several clever approaches have been developed to establish recording synchrony and thereby accurately measure TDOA from widely separated hydrophones. Møhl *et al.* (2000), McGehee (2000), and Wahlberg *et al.* (2001) developed methods that used radiolinked hydrophones to record simultaneous signals on a single recorder. Møhl *et al.* (2001) and Miller and Dawson (2009) used precise GPS timing signals recorded synchronously with the audio recordings from each independent hydrophone to establish a precise time reference. Thode (2004) used two widely spaced elements in linear array and used surface reflections to effectively simulate a large spatial array. Baggenstoss (2011) developed TDOA methods to simultaneously localize multiple individuals. Gassmann *et al.* (2013) described a system for 3D tracking of another species, killer whale (*Orcinus orca*), using a series of several cabled hydrophone arrays suspended from a floating platform.

In many ways, sperm whales are a model species for localization studies. Sperm whales produce loud echolocation clicks with source levels up to 223 dB re: 1  $\mu$ Pa root-mean-square (rms) @ 1 m (Møhl *et al.*, 2000), and even though their clicks are highly directional (Møhl *et al.*, 2000), off-axis signals can be discerned at ranges of several kilometers (Nosal and Frazer, 2007; Miller and Dawson, 2009). Inter-click-intervals are stable and relatively long for sperm whales, which facilitates localization of individuals within groups. Also, their deep-diving behavior makes it difficult to study this species from surface observations alone, which increases the value of passive acoustic methods.

Beaked whales of the family Ziphiidae are also hard-to-study, deep-diving whales, but aspects of their biology and behavior limit the application of the same approaches. Beaked whale echolocation pulses are much higher in frequency (10–90 kHz, Baumann-Pickering *et al.*, 2013) than

those of sperm whales (0.1–20 kHz, Nosal and Frazer, 2007), which prevents the use of off-the-shelf radio equipment to transmit their audio signals to a central recording system. More significantly, the echolocation pulses of the best studied species of beaked whale (Cuvier's beaked whale and Blainville's beaked whale) are highly directional and with an estimated  $-3$  dB beam width of only  $6^\circ$  (Zimmer *et al.*, 2008). Off-axis echolocation signals of Cuvier's beaked whale are estimated to be detectable above ambient noise only to a distance of  $\sim 700$  m (Zimmer *et al.*, 2008). Given that the typical foraging depths of this species is greater than 700 m, only on-axis pulses are likely to be detectable on near-surface hydrophones. Studies with large-aperture arrays of bottom-mounted hydrophones have shown that, due to their narrow beam widths, on-axis pulses are seldom likely to be received simultaneously on a sufficient number of hydrophones to allow localization (Ward *et al.*, 2008).

Several approaches have been developed for 3D acoustic tracking that do not rely on the same signal being received on a widely distributed array of time-synchronized hydrophones. Gassmann *et al.* (2015) used a nested array configuration with two small-aperture, four-element arrays (nodes) nested within a large-aperture array of single-channel recorders for 3D tracking of Cuvier's beaked whales. Each small-aperture array is used to estimate the direction to a sound source in three dimensions, and each hydrophone is recorded on the same instrument, so timing synchrony was not an issue. Although Gassmann *et al.* (2015) established recording synchrony of widely spaced elements by measuring and adjusting for clock drift, their nested method also allows for localization without precise synchronization between recorders. This approach can work even when the same signal is not received at both nodes, so long as signals from the same whale are received by both nodes within a time period that is short enough that animal movement is negligible. DeAngelis *et al.* (2017) used bearing angles from a towed hydrophone array, target motion analysis, and reflected angles to localize several species of beaked whale in the Atlantic. For sperm whales, Nosal and Frazer (2007) avoided the need for precisely synchronized recordings in 3D tracking by utilizing both direct-path and surface-reflected signals received on at least four seafloor hydrophones to localize based on signals received within a 20-s time interval. Methods such as these that do not require the same signal to be received on widely spaced hydrophones and do not require precise time synchronization are ideal for passive acoustic tracking of beaked whales.

Here we present a passive acoustic approach to tracking the 3D diving behavior of whales using a spatial array of unsynchronized hydrophone recorders suspended under drifting buoys. Each node of this large-aperture array is comprised of a vertical array of two closely-spaced (10 m), near-surface hydrophones recorded in stereo. TDOA of echolocation pulses on the vertical arrays are used to estimate detection angles. We test this nested array configuration of a large aperture, unsynchronized spatial array comprised of time-synchronized vertical arrays to study diving behavior of Cuvier's beaked whales in the Catalina Basin, California during two weeks in July and August 2016. Although the same echolocation pulse is seldom received on more than two nodes, pulses are often received on 3–5 nodes

within a relatively short time snapshot, allowing precise localization. We develop a discrete-time, state-space model to track whales using a movement model that constrains travel speed to biologically feasible values and a measurement model that uses the detection angles from multiple vertical arrays. Occasionally available surface reflections provide independent measurements of detection angles and allow correction for small degrees of array tilt. Aspects of diving behavior are inferred from ten estimated 3D dive tracks.

## II. METHODS

We use detection angles measured from a drifting array of hydrophones at  $\sim 100$ -m depth for both localization and tracking of Cuvier's beaked whales. The autonomously recording vertical hydrophone arrays are referred to as drifting acoustic spar buoy recorders (DASBRs). In this paper, we use the term localization to refer to the estimation of a 3D location (in planar space and depth) at a single point in time. As we use this term, localization does not use information from previous or subsequent locations. We use the term tracking to refer to a time series of 3D locations that are estimated in a model. Within the context of the model, estimates of tracking locations are influenced by previous and past locations and can be constrained to realistic values by parameters in the model. Detection angles to the source of a beaked whale echolocation pulse (angular deviation from straight down) are estimated using two methods: (A) the TDOA of a pulse on two elements of a vertical hydrophone array and (B) the TDOA of a pulse and its surface reflection on a single hydrophone. Method A provides an estimate of detection angle from the mid-point of the two elements and is subject to error from array tilt relative to the source; this method is only used in tracking. Method B (often referred to as a virtual array; Cato, 1998) provides an estimate of detection angle that is not affected by array tilt; this method is used in both localization and tracking.

### A. Localization

Localization of a beaked whale in three dimensions at a single point in time is achieved using the TDOA between direct-path and surface-reflected echolocation pulses (method B) received at a minimum of three locations within a short (2-min) time window. Downward conical bearing angles from four points on the sea surface converge exactly at only one point; however, angles from three locations converge at two points and can sometimes provide unambiguous localization if one of those points is implausible (deeper than the seafloor or shallower than the foraging depths of beaked whales). Exact convergence is not guaranteed given measurement error, so we use a maximum likelihood (least-squares) approach to find the best-fit point-of-convergence. Latitude ( $Y$ ) and longitude ( $X$ ) are expressed in kilometers using the Universal Transverse Mercator (UTM) coordinate system. At a beaked whale's horizontal location ( $X, Y$ ), the depth of a point on a downward-opening cone,  $j$ , can be estimated from the location of its apex at the sea surface ( $x_j, y_j$ ) and the detection angle,  $\beta_j$ . For  $\beta_j$  detection angles at  $j$  locations, predicted depths,  $Z_j$  at ( $X, Y$ ) can be estimated as

$$Z_j = R_j / \tan(\beta_j), \quad (1)$$

where  $R_j$ , the horizontal range of ( $X, Y$ ) from apex  $j$ , is estimated as

$$R_j = \sqrt{(X - x_j)^2 + (Y - y_j)^2}. \quad (2)$$

The R (R Core Team, 2013) function *optim* is used to find the position ( $X, Y$ ) that minimizes the sum of squared deviations in the estimated individual and mean ranges (linear fitting methods would work as well)

$$\sum_j \left( R_j - \sum \frac{R_j}{n} \right)^2, \quad (3)$$

where  $n$  is the number of range estimates. We estimate the location of beaked whales using angles estimated only from reflected signals because the measurement of these is not affected by array tilt. We assume that animal movement is small within the 2-min interval used for localizations (see Sec. IV) and ignore a trivially small correction for curvature of the earth.

### B. Tracking

Beaked whale 3D dive tracks are reconstructed using detection angles estimated from at least four DASBRs. Locations in time and space are modeled using a hidden-Markov, state-space model (MacDonald and Zucchini, 1997) in a Bayesian framework. Locations are treated as a latent state constrained by an animal movement model that imposes biological feasibility constraints. Detection angles are used in a measurements model. The model is parameterized with discrete time steps of one minute ( $\Delta t$ ).

Location in space is assumed to be a Markov function of the previous location and velocity vectors. Here we use  $X$  as longitude and  $Y$  as latitude (again in UTM meters) and  $Z$  as depth in meters, and  $X'$ ,  $Y'$ , and  $Z'$  as corresponding velocities. Location at time  $i + 1$  can be specified as

$$X_{i+1} = X_i + X'_i \cdot \Delta t, \quad (4)$$

$$Y_{i+1} = Y_i + Y'_i \cdot \Delta t, \quad (5)$$

$$Z_{i+1} = Z_i + Z'_i \cdot \Delta t. \quad (6)$$

Velocities are specified by an animal movement model that is based on  $x$ - $y$  (horizontal) heading ( $H$ ), vertical pitch ( $P$ ), and speed through the water ( $S$ ).

$$X'_{i+1} = S_{i+1} \cdot \sin(P_{i+1}) \cdot \cos(H_{i+1}), \quad (7)$$

$$Y'_{i+1} = S_{i+1} \cdot \sin(P_{i+1}) \cdot \sin(H_{i+1}), \quad (8)$$

$$Z'_{i+1} = S_{i+1} \cdot \cos(P_{i+1}). \quad (9)$$

Heading, pitch, and speed are estimated from previous values plus normally distributed random deviations ( $\delta$ ) with zero means and standard deviations taken from broad uniform distributions.

$$H_{i+1} = H_i + \delta_H; \quad \delta_H \sim N(\text{mean} = 0, \text{sd} = \sigma_H);$$

$$\sigma_H \sim U(0.05, 1.0); \quad \text{in radians}, \quad (10)$$

$$P_{i+1} = P_i + \delta_P; \quad \delta_P \sim N(\text{mean} = 0, \text{sd} = \sigma_P);$$

$$\sigma_P \sim U(0.0, 1.5); \quad \text{in radians}, \quad (11)$$

$$S_{i+1} = S_i + \delta_S; \quad \delta_S \sim N(\text{mean} = 0, \text{sd} = \sigma_S);$$

$$\sigma_S \sim U(0.1, 0.5); \quad \text{in m s}^{-1}. \quad (12)$$

The state variables are estimated by minimizing the deviations between the observed detection angles for each DASBR and the expected detection angles given the DASBR locations and the state variables. Expected ranges ( $R_{i,j}$ ) at each time step  $i$  to each DASBR  $j$  are estimated as the square root of the sum of squared differences in UTM values of easting and northing [Eq. (2)]. In the animal movement model, predicted detection angles for direct-path ( $\alpha_{i,j}$ ) and reflected-path ( $\beta_{i,j}$ ) angles were calculated from these range estimates, animal depth estimates ( $Z_i$ ), and the mean hydrophone depth of each DASBR ( $D_{i,j}$ ).

$$\alpha_{i,j} = \text{atan}(R_{i,j}/(Z_i - D_{i,j})), \quad (13)$$

$$\beta_{i,j} = \text{atan}(R_{i,j}/Z_i). \quad (14)$$

In the measurement model, predicted angles are modeled as the sum of observed angles ( $O_{i,j}$ ), normally distributed random errors ( $\varepsilon$ ) with zero mean, and, for direct-path angles, a DASBR-specific correction for array tilt ( $T_j$ ).

$$\alpha_{i,j} = O_{i,j} + T_j + \varepsilon_{\alpha j}; \quad \varepsilon_{\alpha j} \sim N(\text{mean} = 0^\circ; \text{sd} = 0.80^\circ), \quad (15)$$

$$\beta_{i,j} = O_{i,j} + \varepsilon_{\beta j}; \quad \varepsilon_{\beta j} \sim N(\text{mean} = 0^\circ; \text{sd} = 0.10^\circ). \quad (16)$$

Array tilt does not affect angles  $\beta$  estimated from surface reflections, so array tilt is assumed to be zero for these angles. In this model,  $\varepsilon$  values represent measurement error and  $T$  values represent bias in the direct-path angles. The standard deviations for  $\varepsilon_\alpha$  and  $\varepsilon_\beta$  are based on a previously measured value for direct-path and reflected angles for DASBRs [standard deviation (sd) = 0.80° and 0.10°, respectively, Barlow and Griffiths, 2017]. The prior distribution for the array tilt correction is modeled as a broad normal distribution with a mean of zero and a standard deviation of 5°.

$$T_j \sim N(\text{mean} = 0^\circ; \text{sd} = 5.0^\circ). \quad (17)$$

The Bayesian posterior distributions of estimated location and other variables are estimated using Markov Chain Monte Carlo (MCMC) algorithms as implemented in OpenBUGS software (Lunn *et al.*, 2009). A short description of this software, alternative methods for fitting state-space models, and the OpenBUGS code for this model are available in the supplemental material.<sup>1</sup> OpenBUGS software is accessed using the *R2OpenBUGS* package v3.2 in R v3.4.2. Estimated parameters include the initial states ( $X_I, Y_I, Z_I, H_I, P_I, S_I$ ), the sds of the normally distributed, zero-mean terms ( $\sigma_H, \sigma_P$ , and  $\sigma_S$ ), and the DASBR-specific values of

the deviations in heading, pitch, and speed between each time step in the model ( $\delta_H, \delta_P$ , and  $\delta_S$ ). Non-informative uniform distributions (Lunn *et al.*, 2012) were used for initial speed, pitch and heading ( $H_I, P_I, S_I$ ). To improve convergence, a plausible initial location ( $X_I, Y_I, Z_I$ ) was determined by trial and error, and this initial location was specified as a normally distributed prior with a standard deviation of 1 km horizontally and 0.3 km vertically. Speeds ( $S_i$ ) are constrained to biologically plausible values (0.25 to 3.5 m s<sup>-1</sup>). Posterior probabilities were based on 200 000 iterations with a thinning ratio of 1:100 after a burn-in of 200 000 iterations (see Lunn *et al.*, 2012 for an explanation of these parameters in OpenBugs).

### C. Array design

Cuvier's beaked whales were localized and tracked using a nested array design comprised of a large aperture array of four to eight drifting nodes. Each node is comprised of a two-element vertical array with hydrophones separated by 10 m and a two-channel autonomous digital recorder (see Fig. 2 in Griffiths and Barlow, 2015). The nodes were deployed initially in two north-south rows with ~900 m separation between rows and between nodes within each row (Fig. 1); however, this array geometry changed during each drift due to random effects of current and wind. Three of our eight recorders failed to record useable data, largely due to problems with underwater connectors, so results presented here will be from arrays with four or five nodes.

One of the five functioning nodes (designated W-4) was based on the design of Griffiths and Barlow (2015, 2016) for a drifting acoustic spar buoy recorder (DASBR v1). It used a Wildlife Acoustics SM2+Bat recorder mounted in a polyvinyl chloride (PVC) spar buoy. Stereo acoustic files were recorded continuously in 5-min WAV-format files at a 192 kHz sample rate. A Kevlar-reinforced underwater Cat-5

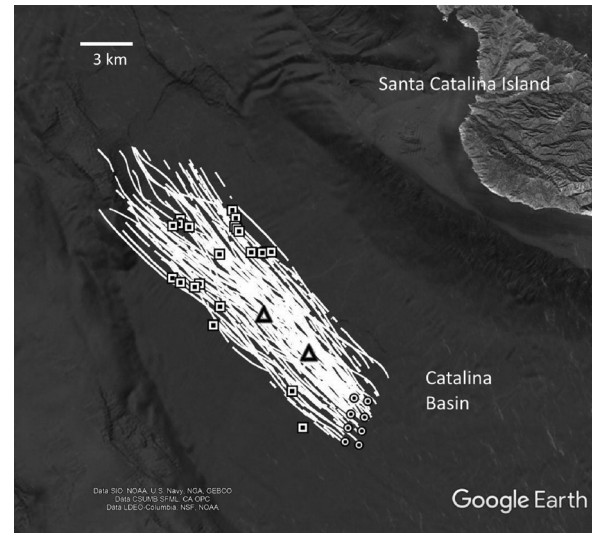


FIG. 1. Drifts of buoy recorders in the Catalina Basin (white lines). Eight buoys were typically deployed in a 2 × 4 rectangular configuration separated by ~900 m (as exemplified by black and white circle symbols) and drifted northeast. Black and white square symbols indicate localized Cuvier's beaked whales (Table I). Drifts were designed to pass over two seafloor recorders (triangles) as part of a different study.

cable (Falmat FMXCAT50000K12) connected two hydrophones (at ~90 m and ~100 m depths) to the floating instrument package. The hydrophones (High Tech, Inc. HTI-96-min) had a sensitivity of  $-182$  dB re:1 V/ $\mu$ Pa and a useable frequency range from 50 Hz to 140 kHz. A differential amplifier in the array added 34 dB of gain. Voltages from a pressure transducer near the hydrophones were recorded by the SM2+Bat recorder to measure depth. A 30-m  $\times$  8-mm elastic cord was attached to the conducting cable to decouple the movement of the surface buoy from the hydrophones. The SM2+Bat signal conditioning settings were zero gain on both channels, a 3 Hz high-pass filter on Channel 0 (upper hydrophone) and a 180 Hz high-pass filter on Channel 1 (lower hydrophone).

The other four functioning nodes (designated B-1 to B-4) used Wildlife Acoustics SM3M autonomous underwater recorders. This configuration (DASBR v2) differed from the previous design in using submersible recorders and a nylon line rather than a near-surface SM2+Bat recorder and a conducting cable. The record duty cycle for the SM3M recorders included a 1-min stereo WAV file at the top of the hour at 96 kHz (for quiet ocean noise measurements), a 5-min sleep period (to force the system clock to synchronize with the temperature-compensated clock), and twenty-seven 2-min WAV files at 256 kHz sampling rate. Two hydrophones (at ~105 m and ~115 m depths) were attached to a nylon line and were connected to the SM3M recorder with 10-m cables. The hydrophones (High Tech, Inc. HTI-96-min) had a sensitivity of  $-165$  dB re:1 V/ $\mu$ Pa and a useable frequency range from 50 Hz to 140 kHz. A 30-m  $\times$  10-mm elastic cord was used immediately below the spar buoy to decouple the movement of the surface buoy from the hydrophones. A 50-m  $\times$  6-mm nylon line was used below the elastic cord, and the SM3M and hydrophones were mounted to a 15-m  $\times$  10-mm nylon line below that. The signal conditioning settings on the SM3M were 12 dB gain on both channels and a 2-Hz high-pass filter on both channels.

The overall configuration was similar for both the DASBR v1 and v2. Two Spot satellite geo-location devices (Gen3 and Trace models, used interchangeably) were mounted in the above-water section of the spar buoys to track and record GPS locations at intervals of 15–30 min. The vertical array orientation was maintained with a 6.5 kg weight at the bottom of each array.

#### D. Field studies

The array of DASBRs was deployed off southern California in the Catalina Basin from 19 July to 1 August 2016. Instruments were initially deployed from the San Diego-based 75-ft dive boat *Horizon*. The array was repositioned 12 times, typically on a daily basis, to re-establish the array geometry using the 25-ft research vessel *Vibrio* from the University of Southern California's Wrigley Marine Science Center. The drifts (Fig. 1) were designed to pass over two High-Frequency Acoustic Recording Packages (HARPs) that were deployed on the seafloor as part of a separate study to compare beaked whale detections among instruments. The midpoint of all drifts was 33.2° N and

118.6° W. Four DASBRs (W-1 to W-4) were removed for data downloading and maintenance from 25 to 27 July. The other four (B-1 to B-4) were removed for data downloading and maintenance from 27 to 28 July.

#### E. Beaked whale identification and bearing angle estimation

Initial processing to identify beaked whale echolocation pulses and estimate direct-path vertical bearing angles used PAMGuard (Beta v1\_15\_03) open-source software<sup>2</sup> (Gillespie *et al.*, 2009). Echolocation signals were detected using the PAMGuard energy-based click detector and were automatically classified by the PAMGuard click classifier into discrete categories based on peak frequency and the presence of a frequency upsweep (Keating and Barlow, 2013). Direct-path, vertical bearing angles were automatically estimated within PAMGuard from the TDOA of the same echolocation pulse on the two elements of the vertical hydrophone arrays which were estimated by cross-correlation of the waveform data. The vast majority of echolocation signals in this area were from dolphins (especially common dolphins which were seen frequently during our field operations). Pulses that were likely to be from Cuvier's beaked whales were initially identified based on having a 22–24 kHz or 34–40 kHz peak frequency, at least occasional upsweeps as determined by the PAMGuard click classifier, and vertical bearing angles from below the array that were relatively consistent over several minutes. Consistent downward bearing angles were the most effective diagnostic for identifying beaked whale echolocation pulses in the presence of larger numbers of dolphin clicks. Characteristics of Cuvier's beaked whale pulses in this area have been described by Baumann-Pickering *et al.* (2014). Likely Cuvier's beaked whale detections were confirmed using four criteria: (1) presence of a clear upsweep in the Wigner plot of high signal-to-noise ratio (SNR) pulses, (2) presence of frequency peaks at 18, 22–24, and 34–40 kHz, (3) presence of a frequency valley or notch at 27 kHz, and (4) inter-pulse intervals greater than 250 ms. In some cases, context-specific information such as the presence of surface reflections and inter-pulse intervals were helpful in confirming species identification (Zimmer and Pavan, 2008). Beaked whales were initially identified by independent analyses of all five DASBRs. If a beaked whale was confirmed on one or more DASBRs, data at that time from the remaining DASBRs were re-examined to determine whether a faint beaked whale may have been missed.

Surface-reflected signals from beaked whales are the sum of incoherent reflections off multiple wave faces, which reduces the precision of cross-correlation methods to estimate bearing angles. Therefore, the precise timing for surface-reflected signals was estimated using the Teager-Kaiser edge-detection approach developed by Barlow and Griffiths (2017). Vertical bearing angles for signals with strong surface reflections were estimated from the TDOA of direct-path and surface-reflected signals.

Estimated bearing angles were corrected for the expected sound speed profile for this month and area. The expected sound speed profile in the Catalina Basin in July at 49 discrete depths between 0 and 1200 m was estimated from temperature and salinity values in the U.S. Navy's Generalized Digital Environmental Model (GDEM-V, version 3.0.1; Carnes, 2009) using the Mackenzie approximation implemented in the function *wasp* in the package *seewave* (Sueur *et al.*, 2008) in R. Direct-path echolocation signals were initially processed in PAMGuard using a sound speed of  $1500 \text{ m s}^{-1}$ , and estimated direct-path bearing angles were adjusted for the expected sound speed at 100 m ( $1490 \text{ m s}^{-1}$ ). The bearing angles for reflected signals were estimated based on the mean sound speed in the top 100 m of the water column ( $1498 \text{ m s}^{-1}$ ). Bearing angle corrections for sound diffraction were estimated using the ray-tracing algorithm in the MATLAB function *raytrace* (Val Schmidt, University of New Hampshire, 2009) based on a beaked whale at an assumed 1000-m depth and at apparent detection angles from  $10^\circ$  to  $80^\circ$  from straight down. The ray-tracing algorithm used interpolated sound speed values at 1-m depth intervals based on a smoothing spline (from the R package *gam*) fit to the above sound speed data at 49 discrete depths. Corrections for diffraction ranged from a low of  $0.04^\circ$  at a detection angle of  $10^\circ$  to a high of  $1.19^\circ$  at  $80^\circ$ .

### III. RESULTS

Individual DASBRs were deployed and retrieved 78 times during the two-week project. The resulting drifts were towards the northwest and generally achieved the objective of drifting over the two seafloor recorders (Fig. 1). Average drift speeds were  $0.76 \text{ km h}^{-1}$  (s.d. =  $0.23 \text{ km h}^{-1}$ ) and, given that the drifts were opposite the direction of the prevailing NW winds, were primarily driven by ocean currents. Twenty-nine dives of Cuvier's beaked whales were identified (see Table S1 in supplemental files).

#### A. Localization

On 23 occasions during eleven of the 29 detected dives, unambiguous localizations could be calculated based on surface reflections received on at least three DASBRs within a 2-min time window (Table I). Localization was not possible for the remaining 18 dives because surface reflections were not detected on at least three DASBRs within this time window. In some cases, two or three localizations were possible within a single dive. The mean estimated depths for these localizations is 977 m (sd = 171 m), and the estimated distances from the localization to the instruments range from 0.43 to 3.48 km (Table I).

TABLE I. Localizations of Cuvier's beaked whales from detection angles estimated from surface-reflected echolocation pulses. Latitude, longitude, and depth are estimated by finding the best convergence of bearing angles from three or more drifting instruments. The minimum and maximum distances from the estimated location to the instruments are also given. Localizations from only three instruments are used only if unambiguously determined (only one solution at plausible depths  $>500 \text{ m}$  and less than the bottom depth).

Dive label	# DASBRs with surface reflections	UTC Date & time	Latitude	Longitude	Depth (m)	Min. distance (km)	Max. distance (km)
AI-1	4	7/22/2016 3:57	33.252	-118.618	1191	1.40	2.49
AI-2	4	7/22/2016 4:24	33.253	-118.610	952	1.42	2.54
AJ-5	3	7/22/2016 6:28	33.247	-118.640	810	0.43	1.42
AP-1	3	7/24/2016 6:16	33.270	-118.634	953	2.16	2.99
AP-1	3	7/24/2016 6:21	33.265	-118.634	854	1.60	2.39
AP-1	3	7/24/2016 6:23	33.264	-118.632	836	1.36	2.17
AR-1	3	7/24/2016 20:30	33.156	-118.556	1193	2.07	3.10
AS-1	4	7/24/2016 23:43	33.176	-118.568	734	1.88	3.45
AW-1	3	7/25/2016 7:54	33.204	-118.633	959	2.52	3.44
AW-1	3	7/25/2016 7:55	33.204	-118.634	925	2.50	3.41
AW-1	3	7/25/2016 8:10	33.216	-118.632	840	1.70	3.43
AY-1	4	7/25/2016 10:57	33.262	-118.674	1085	1.36	2.85
AY-1	4	7/25/2016 11:08	33.259	-118.674	1067	1.34	2.48
AY-1	5	7/25/2016 11:14	33.259	-118.666	1247	1.62	2.80
AY-1	4	7/25/2016 11:20	33.257	-118.678	693	1.12	2.07
BH-1	4	7/26/2016 9:19	33.226	-118.670	976	2.17	3.48
BH-2	4	7/26/2016 9:39	33.225	-118.663	954	1.47	2.62
BL-1	4	7/27/2016 8:11	33.255	-118.604	1169	1.22	2.53
BL-1	4	7/27/2016 8:19	33.254	-118.608	1244	0.87	2.19
BM-2	3	7/27/2016 11:11	33.275	-118.638	671	0.74	1.64
BM-3	4	7/27/2016 11:15	33.263	-118.630	1136	1.03	2.16
BS-1	4	7/29/2016 12:44	33.224	-118.653	1046	1.00	2.46
BS-1	4	7/29/2016 13:07	33.226	-118.650	933	1.26	2.56
Average					977	1.49	2.64
Standard Deviation					171	0.54	0.57
Standard Error					36	0.11	0.12
Maximum					1247	2.52	3.48
Minimum					671	0.43	1.42

TABLE II. Summary statistics for each of ten dive tracks. The net distance traveled is based only on the beginning and ending position of a track, and the net horizontal speed is estimated as the net distance divided by the duration of the track. The rms angle error is the rms difference between the observed direct path angles and those predicted by the fitted track and includes both systematic error due to array tilt and measurement error.

Dive	Duration (min)	Mean speed ( $\text{m s}^{-1}$ )	Mean depth (m)	Maximum depth (m)	Net distance traveled (km)	Net horizontal speed ( $\text{m s}^{-1}$ )	Mean absolute tilt correction (deg)	rms angle error (deg)
AI-1	11	1.18	1035	1323	0.19	0.29	2.22	2.52
AI-2	26	0.64	945	1085	0.79	0.51	1.80	1.92
AI-3	26	0.87	902	1040	0.38	0.24	2.39	3.30
AP-1	32	1.69	879	984	1.59	0.83	0.83	1.02
AR-1	19	1.26	1038	1222	0.96	0.84	1.09	1.37
AS-1	24	0.70	935	984	0.40	0.28	1.11	1.17
AW-1	25	1.57	865	952	1.56	1.04	1.04	1.50
BH-1	11	1.28	911	1001	0.61	0.93	2.46	3.13
BL-1	9	1.14	1240	1286	0.49	0.92	1.14	1.73
BS-1	31	1.61	916	1168	0.71	0.38	2.22	2.39
mean	21.4	1.19	967	1104	0.77	0.63	1.63	2.01
s.d.	8.4	0.37	112	136	0.48	0.31	0.65	0.80

## B. Tracking

Eight of the 11 dives that had localizations were selected for tracking (Table II). In one of those eight dives (AI), tracks of three individuals were sufficiently distinct to allow each to be tracked separately, for a total of ten dive tracks (Table II). In three cases, dives were rejected from analysis because they represented groups of animals whose individual detection angles could not be unambiguously discriminated. Other dives were rejected because they did not have an unambiguous localization from surface reflections or were too short (less than 9 min). The sample includes dive segments from 9 to 32 min duration with an average of 21.4 min (Table II).

Illustrated results are provided for the longest tracked dive (AP-1). The detection angles for the five vertical hydrophone arrays (Fig. 2) steadily decline from the start until

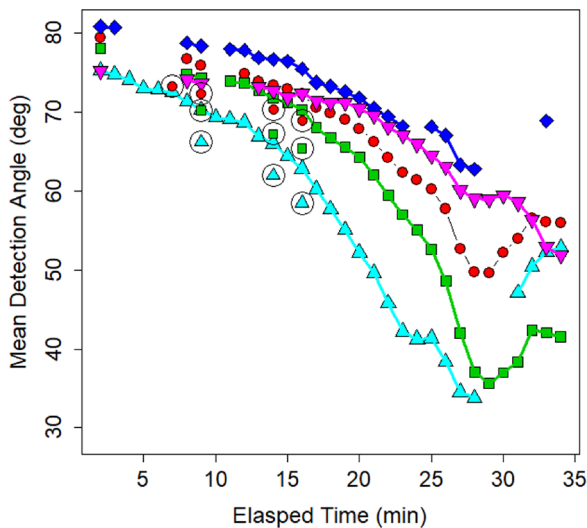


FIG. 2. (Color online) Detection angles (relative to vertical) of beaked whale echolocation pulses measured from the TDOA from dive “AP-1” received by a vertical hydrophone array of each DASBR (filled symbols). Symbols and colors correspond to the same DASBR drifts illustrated in Fig. 3. Detection angles for reflected signals are circled and those for direct-path signals are not circled. Detection angles are averaged over 1-min intervals and are not available for all minutes.

27 min elapsed time, indicating that the whale and the DASBR array were getting closer. This is also seen in the estimated track [Fig. 3(A)]. At 27 min, the whale turns away from four of the vertical arrays but continues toward the fifth

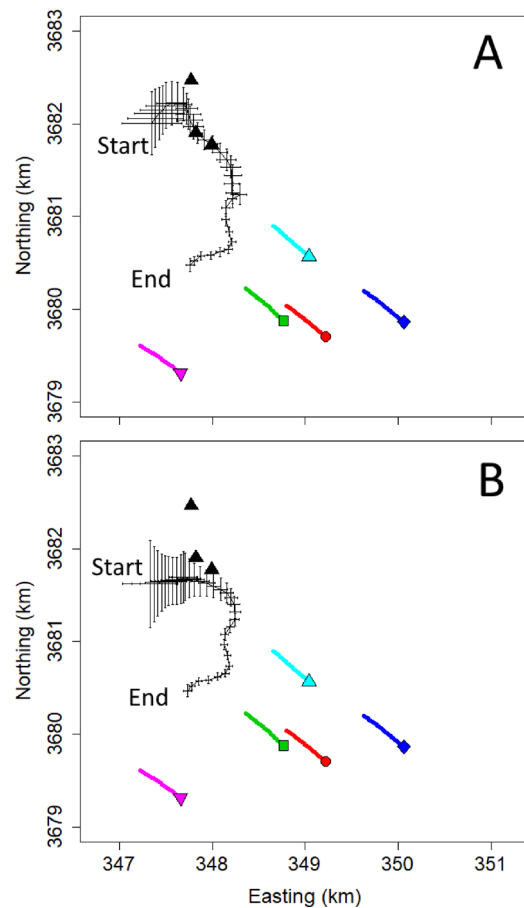


FIG. 3. (Color online) DASBR drifts (colored lines) and estimated spatial tracks of beaked whales (black line with error bars) during a 32-min period of echolocation for dive AP-1 with (A) and without (B) correction for array tilt. Localizations based on surface reflections are illustrated as black triangles. Location error bars indicate two standard deviations from the Bayesian posterior distributions. Symbols and colors at the start of each DASBR drift correspond to symbols in Fig. 2. Coordinates are for Zone 11 of the Universal Transverse Mercator system.



(Figs. 2–3). The three localizations from reflected angles are generally in good agreement ( $\pm 100$  m) with the estimated track locations. The estimated depth during this track varied from 750 to 950 m. Swim speed during this dive approached  $2.5 \text{ m s}^{-1}$ , and the mean speed ( $1.7 \text{ m s}^{-1}$ ) was the fastest estimated for the ten tracks (Table II).

During track AP-1, the mean estimated angular correction for array tilt was  $0.83^\circ$  for the five DASBRs. If array tilt is assumed to be zero, the estimated track is shifted in space by  $\sim 0.5$  km at the beginning of the track, but this track error becomes almost trivial when the animal is closer to the recorders [Fig. 3(B)]. Without tilt correction, the track does not pass as near the localizations which are based on reflected angles [Fig. 3(B)]. Also, in this case, the initial depth is shallower ( $\sim 600$  m) and swimming speeds are lower without tilt correction.

The mean depth of all tracks is 967 m, but varies considerably among individual tracks (Fig. 4). The overall mean swim speed is  $1.19 \text{ m s}^{-1}$  with a range from 0.6 to  $1.7 \text{ m s}^{-1}$  among tracks (Table II). Swim directions show no obvious patterns and, in three cases, changed markedly during a dive (Fig. 5). The mean net horizontal speed ( $0.63 \text{ m s}^{-1}$ ) is roughly half the mean swim speed. The angular corrections for array tilt have a mean absolute value of  $1.6^\circ$  (Table II). Detailed plots for all ten tracks are given in supplemental material.

In one case (dive AI), tracks of multiple individuals were sufficiently distinct to allow each to be tracked individually, and dives from three individuals (or tightly associated subgroups) in this “group dive” are included separately in the sample of ten tracked dives. Dive AI had the longest period of echolocation (53 min) of all the identified dives. Track AI-1 consisted of a steep dive towards the bottom and ended at about the same time that tracks AI-2 and AI-3 began, again as descents that ended at approximately 1000–1100 m depth.

## IV. DISCUSSION

### A. Swimming speed

The swimming speed of Cuvier’s beaked whales during foraging dives has not been directly measured from tagging

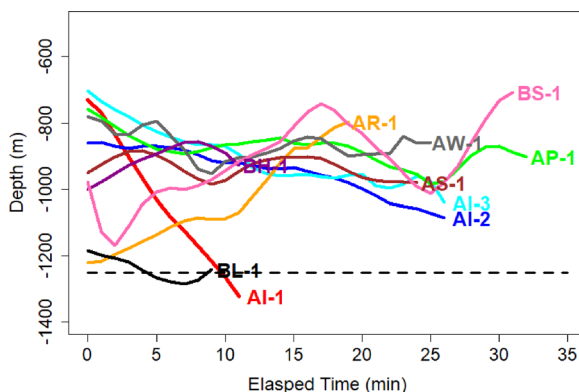


FIG. 4. (Color online) Estimated depths for ten tracked beaked whale dives. Labels indicate specific dives or segments of dives (Table II). Dashed black line indicates nominal seafloor depth in the Catalina Basin.

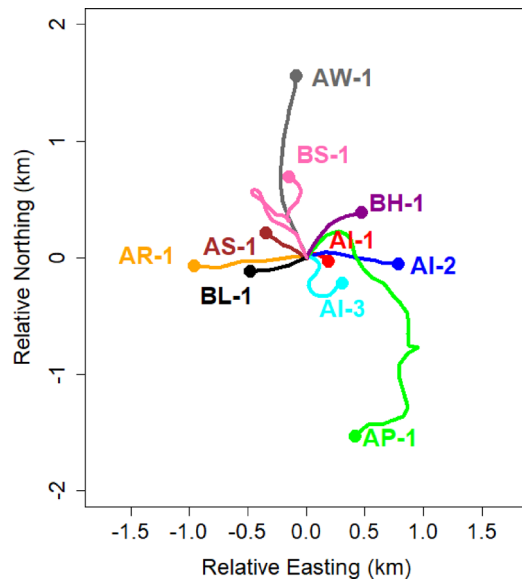


FIG. 5. (Color online) Track locations for ten tracked beaked whale dives relative to their start location (at the origin: 0, 0). End locations are indicated with filled circles. Labels at end locations indicate specific dives or segments of dives (Table II).

studies, but rapid avoidance speeds were estimated as  $2.6$  and  $3.1 \text{ m s}^{-1}$  (DeRuiter *et al.*, 2013). The descent and ascent rates for a deep dive have been measured as  $1.5$  and  $0.7 \text{ m s}^{-1}$  (respectively) in the Ligurian Sea (Tyack *et al.*, 2006) and  $1.4$  and  $0.68 \text{ m s}^{-1}$  (respectively) off Hawaii (Baird *et al.*, 2008); however, these are based on rates of change in depth and are not true swim speeds. From accelerometers within their tags, Tyack *et al.* (2006) estimate a mean decent angle of  $72^\circ$  and an ascent angle of  $35^\circ$  during deep dives. Based on these, the expected swim speeds would be  $1.5$ – $1.6 \text{ m s}^{-1}$  on descent and  $\sim 1.2 \text{ m s}^{-1}$  on ascent. The Gassmann *et al.* (2015) tracking study estimated horizontal movement speeds ranging from  $1$  to  $3 \text{ m s}^{-1}$ . The swim speeds estimated in our dive tracking study (mean =  $1.18 \text{ m s}^{-1}$ ) are consistent with those from these previous studies of foraging behavior and are much less than speeds that have been measured during avoidance behavior. However, our estimates of swim speeds are based on net movements in 1-min time intervals and do not include the potential of course changes within that interval which would result in a slight underestimate of true foraging speeds.

### B. Foraging times

Because Cuvier’s beaked whales typically produce echolocation pulses only during deep dives (Tyack *et al.*, 2006), the duration of a period of regular pulses can be used to infer the duration of a foraging bout. In this study, it is clear that echolocation pulses cannot always be received by all hydrophones, even at relatively close range. For dive AP-1 (Fig. 2), echolocation pulses were received more consistently after 10 min from the start, when the animal turned towards the drifting array of hydrophones. Pulse reception became intermittent again when the animal turned away from some hydrophones at 29 min. Because reception of

echolocation pulses varies with animal orientation and range, we cannot precisely estimate foraging times with our data.

The expected duration of the foraging portion of a deep dive can be estimated from previous tagging studies. Acoustic tagging studies have shown that regular echolocation pulses start at an average depth of 457 m on descent and ends at a depth of 856 m on ascent. Based on mean descent and ascent rates of 1.45 and 0.69 m s<sup>-1</sup> (averaged from the studies cited above), echolocation pulses would begin approximately 5.3 min after the start of a deep dive and would end approximately 20.7 min before the end of the dive. If the same pattern holds elsewhere, foraging times would be approximately 26 min less than deep dive times. From tagging studies, the mean duration of deep dives has been estimated as 58 min (sd = 11 min) in the Ligurian Sea (Tyack *et al.*, 2006), 68 min (sd = 9 min) off Hawaii (Baird *et al.*, 2008), and 67 min (sd = 6.9) off southern California (Schorr *et al.*, 2014). Based on these total dive times, the expected time foraging would be 32, 42, and 41 min (respectively). Warren *et al.* (2017) directly measured the duration of echolocation bouts in California (35.1 min, sd = 9.1) and the Ligurian Sea (35.2 min, sd = 5.7). Most of the echolocation periods on dives in this study (17 of 29) were shorter than 20 min and likely represent fragments of dives when the animal's range and orientation allowed detection of their echolocation signals. However, 8 of these 29 identified dives had echolocation periods longer than 30 min and represent a substantial portion of the expected foraging time during a deep dive.

### C. Dive depths

The mean value of maximum depth per dive for the ten tracks in our study (1104 m) is similar to the mean for Cuvier's beaked whale dives from tagging studies in the Ligurian Sea (1070 m, Tyack *et al.*, 2006), but is not as deep as measured for tagged whales off Hawaii (1392 m, Baird *et al.*, 2008) and elsewhere off southern California (1401 m, Schorr *et al.*, 2014). Beaked whale dives in the Catalina Basin are constrained by the depth of that basin (~1250 m), which explains some of this difference. Although some animals in this study were foraging on or near the bottom during at least a portion of their dive (dives AI-1, AR-1, and BL-1, Fig. 4), the majority of echolocation signals were not near the seafloor. Dives AI-1 and BL-1 appear to go below the nominal seafloor depth (Fig. 4); however, the confidence limits of these estimated depths include the estimated seafloor depth.

In our study, the mean depth of foraging is 967 m [sd = 112 m, standard error (s.e.) = 35.4 m]. In a study area only ~100 km south and in similar water depths, the Gassmann *et al.* (2015) study found a mean foraging depth of 1041 m (sd = 140.3 m, s.e. = 42.3 m, Gassmann, 2018). Mean foraging depth has not been reported for tagged animals, but Baird *et al.* (2008) reports that the mean depth when deeper than 800 m in Hawaii is 1282 m. DeAngelis *et al.* (2017) found an average depth for Cuvier's beaked whales detected with towed arrays off the U.S. Atlantic coast to be 1158 m (sd = 287 m). Acoustic tags in the Ligurian Sea

(Tyack *et al.*, 2006) and tracking studies using bottom-mounted hydrophones in Southern California (Gassmann *et al.*, 2015) show that Cuvier's beaked whales start echolocation at a depth of ~500 m during their descent. None of the localizations or tracks in our study were above 600 m and only two localizations were above 700 m. Although this may indicate that echolocation starts at deeper depths in our study area, this is likely an artifact of animal orientation. The declination angle during descent has been estimated as 72° (Tyack *et al.*, 2006), hence the main axis of their echolocation signals will be facing away from our hydrophones at 100-m depth. Near-surface hydrophones may simply be less likely to detect beaked whales during the descent phase of their deep dives.

### D. Foraging strategies

Few of the individuals in this study appear to concentrate their foraging on or near the seafloor. Clearly, the seafloor at 1250 m is within the foraging depth range of Cuvier's beaked whales; however, it appears to be used only occasionally by a few individuals. Similarly, in Gassmann *et al.* (2015), their Fig. 6(a) also showed that a Cuvier's beaked whale in southern California spent most of its time foraging ~300–400 m above the seafloor.

Our tracking data show that beaked whales can be detected on near-surface hydrophones at horizontal ranges greater than 1 km even when their net direction of travel is away from the hydrophone (Fig. 3). Previous propagation modeling by Zimmer *et al.* (2008) indicated that off-axis echolocation pulses are unlikely to be detected at slant ranges greater than 0.7 km. The most likely explanation for our observation is that beaked whales are not limiting their acoustic search to waters directly ahead of their net direction of travel. Our estimates of net horizontal speed of tracked whales is roughly half of their estimated swim speeds. Although some whales traveled in relatively straight lines (Fig. 5), their net horizontal speeds were still less than their mean estimated swim speeds (Table II), likely because they are turning frequently while foraging and because swim speed can have a vertical vector component. The net direction of travel underwater appeared to be random with respect to the direction of the northwesterly surface currents (Fig. 5). At 0.63 m s<sup>-1</sup>, the net horizontal distance covered on a typical 40 min foraging bout would be ~1.5 km.

### E. Group foraging behavior

In most groups of Cuvier's beaked whales, individuals proved difficult to track because their detection angles plotted against time appeared so inter-braided that individuals could not be discriminated. In only one case (dive AI), detection angles appeared to be sufficiently distinct to identify three individuals or closely associated subgroups. At the one point in time when echolocation pulses from all three overlapped, they appeared to be separated by ~200–400 m. This dive period was the longest measured bout of echolocation (53 min), possibly because one subgroup (AI-1) began descending before the other two. The acoustic tracking by Gassmann *et al.* (2015) also showed separations of hundreds

of meters between individuals within groups of Cuvier's beaked whales, with occasional convergences of individuals during a dive.

Group foraging behavior could be better studied with a different study design. If recorders were precisely synchronized, individual echolocation pulses might be localized, and the methods used by Gassmann *et al.* (2015) could be used to assign pulses and locations to specific individuals. Given that individuals can be precisely localized from surface reflections, time synchronization among recorders may be possible using echolocation pulses as timing signals.

## F. Localization and tracking

This study has shown the feasibility of using echolocation pulses for localization and tracking of Cuvier's beaked whales. The combination of localization using surface-reflected signals and tracking using the more frequent direct-path signals allows some degree of correction for array tilt that would otherwise bias the estimated whale locations. However, the approach used here is a rather crude approximation. Array tilt has two components: an absolute value and an azimuth relative to the direction of the animals. With our approach, we estimate a single tilt correction as an additive error in direct-path detection angle for each DASBR. In reality, that correction should depend on the bearing to the animal relative to the azimuth of the array tilt. This underspecification of the problem likely explains why one of the localizations in Fig. 3 does not fall precisely on the estimated animal track. Ideally, we would estimate both the absolute value and the azimuth of the array tilt, but we did not receive reflected signals often enough to allow estimation of both parameters. In the future, we recommend precisely measuring the absolute value of array tilt directly with 3D accelerometers fixed rigidly to each array and then estimating only the azimuth term in the tracking model.

Because surface-reflected signals were relatively rarely detected, reflected detection angles were averaged within a 2-min time window to increase the sample size for localization and for correcting array tilt in the tracking algorithm. However, based on an average speed of  $1.2 \text{ m s}^{-1}$ , this introduces potential location errors of  $\sim 144 \text{ m}$ . This factor, more than any other, likely determines the absolute track accuracy. For this reason, direct path angles were averaged over a shorter 1-min time window. Although a shorter time window might improve relative accuracy of the track, the longer 2-min window for reflected angles will still limit the absolute track accuracy. Two approaches could improve track accuracy. If array tilt could be eliminated by using heavier weights and larger sub-surface buoys, the need for reflected angles would be eliminated, and localization could be based solely on direct-path angles. Alternatively, a single recording hydrophone near the surface (say a 10-m depth) might be able to more frequently detect surface reflected signals and allow for a shorter averaging window.

## V. CONCLUSION

We have shown that acoustic localization and tracking using drifting near-surface hydrophones can be an alternative

to tagging for the study of beaked whale diving behavior. Results from this study are generally consistent with results from tagging studies in southern California and other areas. We were able to measure diving behavior from ten tracks in a study that lasted just two weeks. A previous study (Gassmann *et al.*, 2015) showed that beaked whales could also be tracked using bottom-mounted recorders. Many more echolocation pulses can be detected if the hydrophones are within the foraging plane of the whales (1000–1300 m depth) because more of the echolocation signals will be on-axis and detectable at greater distances. However, in most of the world's oceans, the seafloor is much farther from this optimum foraging depth than is the surface, thus beaked whale tracking with near-surface hydrophones is more generally applicable to all the world's oceans than tracking with bottom-mounted hydrophones. Our approach using near-surface hydrophones only requires measurement of declination angles and thus only requires pairs of hydrophones in a vertical array to be precisely time-synchronized. The Gassmann *et al.* (2015) method requires at least two 4-channel volumetric arrays that are precisely aligned and (internally) time-synchronized. Nested hydrophone arrays in both drifting and bottom-mounted configurations appear to be viable options for tracking beaked whale foraging behavior, and the optimum method is likely to vary with local conditions.

Acoustic tracking cannot be viewed as a replacement for tagging studies. Tagging provides information about the diving behavior of beaked whales when they are not vocalizing, which acoustic tracking cannot do. Also, information from pressure sensors, accelerometers, and magnetometers on tags provides much more detailed information on diving behavior than our tracking data. However, despite considerable tagging effort, tagging studies have been largely limited to a few of the 22 species of beaked whale. In part, this is because the other species either do not occur in calm, near shore areas where tagging is feasible or because they do not occur in high densities. Even in calm conditions in high density areas, one or two weeks of dedicated effort may be needed to place a tag on a single individual.

We hope that acoustic tracking will be used as an alternative to tagging to study beaked whale behavior for some of the species for which tagging has not been successful. We do not know much about the diving habits of the vast majority of beaked whale species. Some only live in far offshore areas where surface conditions are often too rough for tagging. In such studies, additional effort should be considered to precisely time-synchronize the recorders and thereby obtain more information to allow tracking individuals within a group.

In addition to their use in localization and tracking, drifting recording systems have many other uses in studies of cetacean behavior, distribution, and abundance. In a larger-scale study, DASBRs have been used to identify a new beaked whale echolocation pulse type (Griffiths *et al.*, in press) and to map the distribution of this and other known beaked whale pulse types in the California Current (Keating *et al.*, 2018). Drifting buoy systems can be used to study distribution and relative abundance of cetaceans in ocean basins

where seafloor hydrophone recorders are impractical or ineffective due to the depth of the seafloor. Ultimately, we hope to use drifting hydrophone recorders to estimate the density and abundance of beaked whales, sperm whales, and other cetacean species.

## ACKNOWLEDGMENTS

Funding for this research was provided by the U.S. Office of Naval Research (Project Nos. N00014-15-1-2142 and MIPR N0001416IP00059) and NOAA's Southwest Fisheries Science Center. Vessel time on the Horizon was funded by NOAA's Cooperative Research Program. Funding for DASBR development and some equipment was provided by the U.S. Navy's N45 and Living Marine Resource programs and by NOAA's Acoustics Program. We thank Mike Weise, Frank Stone, Jason Gedamke, Lisa Ballance, and Anu Kumar for their support. Field assistance was provided by Selene Fregosi, Dave Mellinger, Jennifer Keating, and Eiren Jacobson. Vessel operators were Trevor Oudin, Juan Carlos Aguilar, and Spencer Salmon. The Bayesian tracking algorithm was inspired by OpenBUGS code published by Laplanche *et al.* (2015). Jeff Moore helped in implementing the R2OpenBUGS package. This manuscript was improved by helpful reviews from Jeff Moore, Selene Fregosi, and three anonymous reviewers.

<sup>1</sup>See supplementary material at <https://doi.org/10.1121/1.5055216> for a more detailed table with times and durations of all acoustically detected foraging dives, BUGS code for the tracking algorithm, and additional color plots illustrating the detection angles,  $x$ - $y$ - $z$  locations, and speeds for all ten tracked dives.

<sup>2</sup><https://www.pamguard.org/>.

- Baggenstoss, P. M. (2011). "An algorithm for the localization of multiple interfering sperm whales using multi-sensor time difference of arrival," *J. Acoust. Soc. Am.* **130**, 102–112.
- Baird, R. W., Webster, D. L., Schorr, G. S., McSweeney, D. J., and Barlow, J. (2008). "Diel variation in beaked whale diving behaviour," *Mar. Mam. Sci.* **24**, 630–642.
- Barlow, J., and Griffiths, E. T. (2017). "Precision and bias in estimating detection distances for beaked whale echolocation clicks using a two-element vertical hydrophone array," *J. Acoust. Soc. Am.* **141**, 4388–4397.
- Baumann-Pickering, S., McDonald, M. A., Simonis, A. E., Berga, A. S., Merckens, K. P. B., Oleson, E. M., Roch, M. A., Wiggins, S. M., Rankin, S., Yack, T. M., and Hildebrand, J. A. (2013). "Species-specific beaked whale echolocation signals," *J. Acoust. Soc. Am.* **134**, 2293–2301.
- Baumann-Pickering, S., Roch, M. A., Brownell, R. L., Jr., Simonis, A. E., McDonald, M. A., Solsona-Berga, A., Oleson, E. M., Wiggins, S. M., and Hildebrand, J. A. (2014). "Spatio-temporal patterns of beaked whale echolocation signals in the North Pacific," *PLoS one* **9**(1), e86072.
- Carnes, M. R. (2009). "Description and evaluation of GDEM-V 3.0," Naval Research Laboratory Memorandum Report NRL/MR/7330-09-9165, NRL, Washington, D.C.
- Cato, D. H. (1998). "Simple methods of estimating source levels and locations of marine animal sounds," *J. Acoust. Soc. Am.* **104**, 1667–1678.
- DeAngelis, A. I., Valtierra, R., Van Parijs, S. M., and Cholewiak, D. (2017). "Using multipath reflections to obtain dive depths of beaked whales from a towed hydrophone array," *J. Acoust. Soc. Am.* **142**, 1078–1087.
- DeRuiter, S. L., Southhall, B. L., Calambokidis, J., Zimmer, W. M. X., Sadykova, D., Falcone, E. A., Friedlaender, A. S., Joseph, J. E., Moretti, D., Schorr, G. S., Thomas, L., and Tyack, P. L. (2013). "First direct measurements of behavioral responses by Cuvier's beaked whales to mid-frequency active sonar," *Biol. Lett.* **9**, 20130223.
- Gassmann, M. (2018). (private communication).
- Gassmann, M., Henderson, E., Wiggins, S. M., Roch, M. A., and Hildebrand, J. A. (2013). "Offshore killer whale tracking using multiple hydrophone arrays," *J. Acoust. Soc. Am.* **134**, 3513–3521.
- Gassmann, M., Wiggins, S. M., and Hildebrand, J. A. (2015). "Three-dimensional tracking of Cuvier's beaked whales' echolocation sounds using nested hydrophone arrays," *J. Acoust. Soc. Am.* **138**, 2483–2494.
- Gillespie, D., Mellinger, D. K., Gordon, J., McLaren, D., Redmond, P., McHugh, R., Tinder, P., Deng, X.-Y., and Thode, A. (2009). "PAMGUARD: Semiautomated, open source software for real-time acoustic detection and localisation of cetaceans," *J. Acoust. Soc. Am.* **125**, 2547.
- Griffiths, E. T., and Barlow, J. (2015). "Equipment performance report for the drifting acoustic spar buoy recorder (DASBR)," NOAA Technical Memorandum NOAA-TM-NMFS-SWFSC-543, NOAA, Silver Spring, MD.
- Griffiths, E. T., and Barlow, J. (2016). "Cetacean acoustic detections from free-floating vertical hydrophone arrays in the southern California current," *J. Acoust. Soc. Am.* **140**(5), EL399–EL404.
- Griffiths, E. T., Keating, J. L., Barlow, J., and Moore, J. E. (2018). "Description of a new beaked whale echolocation pulse type in the California Current," *Mar. Mam. Sci.* (in press).
- Johnson, M., Hickmott, L. S., Aguilar Soto, N., and Madsen, P. T. (2008). "Echolocation behavior adapted to prey in foraging Blainville's beaked whale (*Mesoplodon densirostris*)," *Proc. R. Soc. B* **275**, 133–139.
- Johnson, M., Madsen, P. T., Zimmer, W. M. X., Aguilar de Soto, N., and Tyack, P. L. (2004). "Beaked whales echolocate on prey," *Proc. R. Soc. Lond. B* **271**(Suppl 6), S383–S386.
- Keating, J. L., and Barlow, J. (2013). "Click detectors and classifiers used during the 2012 southern California behavioral response study," NOAA Technical Memorandum NOAA-TM-NMFS-SWFSC-517, NOAA, Silver Spring, MD.
- Keating, J. L., Barlow, J., Griffiths, E. T., and Moore, J. E. (2018). "Passive acoustics survey of cetacean abundance level (PASCAL-2016) Final Report, Honolulu (HI)," US Department of the Interior, Bureau of Ocean Energy Management OCS Study BOEM 2018-025, Washington, D.C.
- Laplanche, C., Marques, T. A., and Thomas, L. (2015). "Tracking marine mammals in 3D using electronic tags," *Methods Ecol. Evol.* **6**, 987–996.
- Lunn, D., Jackson, C., Best, N., Thomas, A., and Spiegelhalter, D. (2012). *The BUGS Book: A Practical Introduction to Bayesian Analysis* (CRC Press, Boca Raton, FL), p. 399.
- Lunn, D., Spiegelhalter, D., Thomas, A., and Best, N. (2009). "The BUGS project: Evolution, critique and future directions (with discussion)," *Stat. Med.* **28**, 3049–3082.
- MacDonald, I. L., and Zucchini, W. (1997). *Hidden Markov and Other Models for Discrete-Valued Time Series. Monographs on Statistics and Applied Probability* (Chapman and Hall, London), Vol. 70, p. 236.
- McGehee, D. E. (2000). "Simple methods for locating, counting, and tracking sperm whales underwater in three dimensions," *J. Acoust. Soc. Am.* **108**, 2540.
- Miller, B., and Dawson, S. (2009). "A large-aperture low-cost hydrophone array for tracking whales from small boats," *J. Acoust. Soc. Am.* **126**, 2248–2256.
- Möhl, B., Wahlberg, M., and Heerfordt, A. (2001). "A large-aperture array of nonlinked receivers for acoustic positioning of biological sound sources," *J. Acoust. Soc. Am.* **109**, 434–437.
- Möhl, B., Wahlberg, M., Madsen, P. T., Miller, L. A., and Surlykke, A. (2000). "Sperm whale clicks: Directionality and source level revisited," *J. Acoust. Soc. Am.* **107**, 638–648.
- Nosal, E.-M., and Frazer, L. N. (2007). "Sperm whale three-dimensional track, swim orientation, beam pattern, and click levels observed on bottom-mounted hydrophones," *J. Acoust. Soc. Am.* **112**, 1969–1978.
- R Core Team. (2013). "R: A language and environment for statistical computing," R Foundation of Statistical Computing, Vienna, Austria, <http://www.R-project.org/> (2018).
- Schorr, G. S., Falcone, E. A., Moretti, D. J., and Andrews, R. D. (2014). "First long-term behavioral records from Cuvier's beaked whales (*Ziphius cavirostris*) reveal record-breaking dives," *PLoS One* **9**, e92633.
- Sueur, J., Aubin, T., and Simonis, C. (2008). "Seewave: A free modular tool for sound analysis and synthesis," *Bioacoustics* **18**, 213–226.
- Thode, A. (2004). "Tracking sperm whale (*Physeter macrocephalus*) dive profiles using a towed passive acoustic array," *J. Acoust. Soc. Am.* **116**, 245–253.

- Tyack, P. L., Johnson, M., Soto, N. A., Sturlese, A., and Madsen, P. T. (2006). "Extreme diving behaviour of beaked whales," *J. Exp. Biol.* **209**, 4238–4253.
- Visser, F. (2017). (private communication).
- Wahlberg, M., Møhl, B., and Madsen, P. T. (2001). "Estimating source position accuracy of a large-aperture hydrophone array for bioacoustics," *J. Acoust. Soc. Am.* **109**, 397–406.
- Ward, J., Morrissey, R., Moretti, D., DiMarzio, N., Jarvis, S., Johnson, M., Tyack, P., and White, C. (2008). "Passive acoustic detection and localization of *Mesoplodon densirostris* (Blainville's beaked whale) vocalization using distributed bottom-mounted hydrophones in conjunction with a digital tag (DTAG) recording," *Can. Acoust.* **36**, 60–66.
- Warren, V. E., Marques, T. A., Harris, D., Thomas, L., Tyack, P. L., Aguilar de Soto, N., Hickmott, L. S., and Johnson, M. P. (2017). "Spatio-temporal variation in click production rates of beaked whales: Implications for passive acoustic density estimation," *J. Acoust. Soc. Am.* **141**, 1962–1974.
- Zimmer, W. M., Harwood, J., Tyack, P. L., Johnson, M. P., and Madsen, P. T. (2008). "Passive acoustic detection of deep diving beaked whales," *J. Acoust. Soc. Am.* **124**, 2823–2832.
- Zimmer, W. M., and Pavan, G. (2008). "Context driven detection/classification of Cuvier's beaked whale (*Ziphius cavirostris*)," in *Proceedings of the New Trends for Environmental Monitoring Using Passive Systems Conference 2008*, October 14–17, Hyeres, France, pp. 1–6.